

# Reactor Vibration Analysis in Consideration of Coupling between the Magnetic Field and Vibration

Tetsuhiro Ishikawa Hiroo Sugiyama  
TOYOTA MOTOR Co, Ltd.

Emiko Baba  
TOYOTA TECHNO SERVICE Co, Ltd.

Ryusuke Oka  
TOYOTA COMMUNICATION SYSTEM Co, Ltd.

Yoshihiro Kawase  
GIFU University

Yutaka Suzuki  
NIPPON SOKEN, INC.

Michio Tatsuno  
TOKYO SEIDEN Co, Ltd.

This paper describes how the cause of noise in a hybrid vehicle reactor was elucidated by the development of technology to analyze the coupling between the magnetic field and vibration in the high-frequency range (5 to 10 kHz) and how reactor noise was reduced as a result.

To date, magnetic field and vibration analyses, for reactors have been done but mainly within conditions at the commercial frequency range (around 60 Hz).[1], [2], [3]

This paper describes how the reactor behavior in the high-frequency range (5 to 10 kHz) was clarified by constructing a suitable model and analyzing electromagnetic fields and vibration phenomena occurring in it. Actual measurements were also used for the analyses.

In addition, this analytical technique was used to elucidate the cause of noise and to develop a new form of reactor to reduce noise. As a result, noise was reduced by 10 dB or more.

*Keywords – coupled analysis, reactor design and simulation, dc/dc converters*

## I. INTRODUCTION

The hybrid vehicle reactor is a functional part supplying higher voltage to the motor and smoothing the current. It is used in combination with a step-up chopper circuit. (Fig. 1)

The same type of reactor is also used for the DC/DC converter that is installed in the fuel cell hybrid vehicle, which uses a combination of two power sources: fuel cells and a secondary battery. (Fig. 2)

The reactor should be made compact but decreasing the reactor size increases the magnetic flux density, which increases electromagnetic force and magnetic strain, thereby increasing vibration. This vibration propagates to the vehicle body causing noise within the vehicle, which can be a problem. The reactor is used at high frequencies (5 to 10 kHz) in order to reduce power loss and improve response. The higher frequency makes the noise easily audible and unpleasant. In order to solve these problems related to vibration and noise, a technique to analyze the coupling between the electromagnetic force and the vibration at high frequencies had to be constructed.

Analyses of magnetic fields and vibration of the reactor have been carried out for more than twenty years, mainly for power converters. Coupled analyses have also been done in recent years, but these have mainly been carried out at commercial frequencies, and no analyses have been done in the frequency range above 10 kHz.

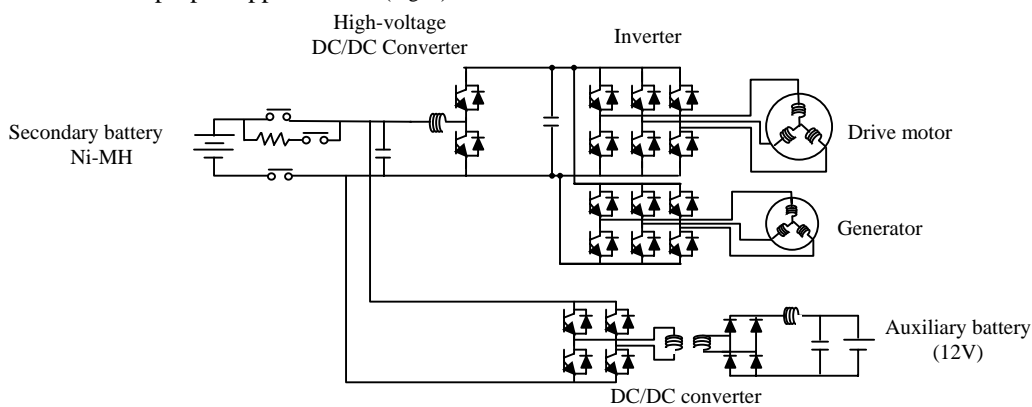


Fig.1 THS- High-voltage System Configuration

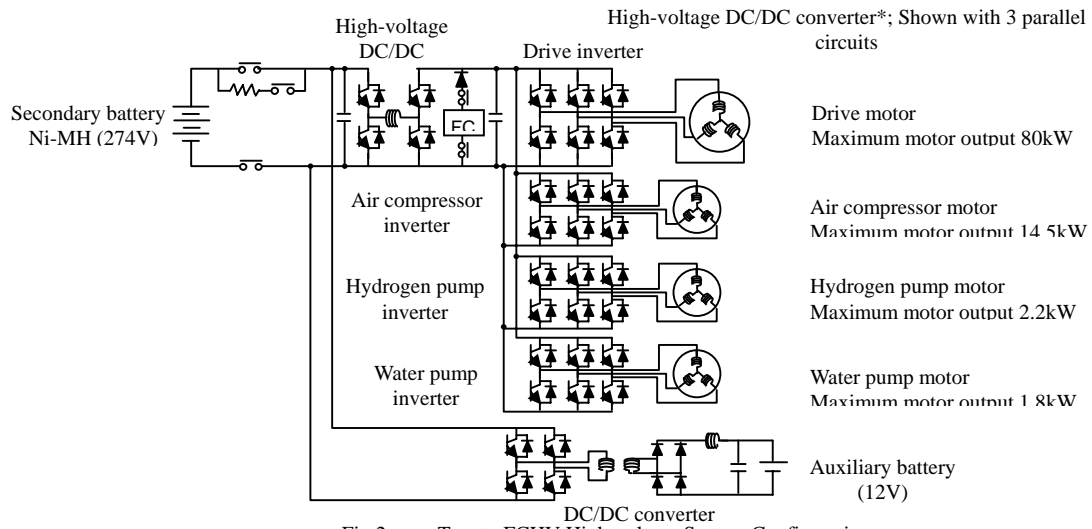


Fig.2 Toyota FCHV High-voltage System Configuration

In this study of the high-frequency range above 10 kHz, a technology was developed to analyze the electromagnetic force and vibration of the reactor, and the results were compared with measurements. A prototype reactor was also built that uses this analytical technique to reduce vibration, and the results for the prototype are also described here.

## II. STRUCTURE AND FUNCTION OF REACTOR

Fig.3 shows an exterior view of the reactor. Gaps are built in the reactor's iron core in order to maintain a fixed current smoothing action (a fixed inductance) across a wide range of input currents. The gaps maintain the fixed inductance by intentionally increasing the magnetic resistance and to inhibit magnetic saturation.

The electrical specifications for the reactor that was analyzed in this study are shown in TABLE I.

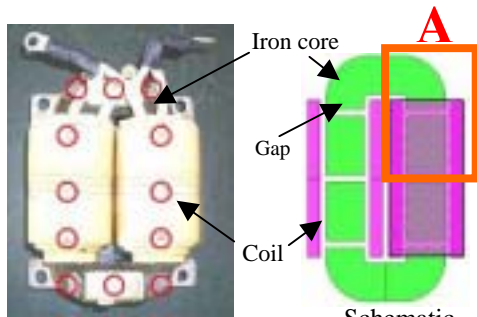


Fig.3 Reactor Exterior View

TABLE I. REACTOR'S ELECTRICAL SPECIFICATIONS

<b>Inductance</b>		290 ± 25 μH
<b>Modulation frequency (Carrier frequency)</b>		9.6kHz
<b>Passed current value</b>	<b>Maximum</b>	77.5A
	<b>Minimum</b>	12.5A
<b>Input voltage</b>		288V
<b>Output voltage</b>		650V

## III. ANALYSIS METHOD

The vibration that arises in the reactor was thought to be caused by the electromagnetic force that acts over the gap parts. Then the vibration was thought propagate to the fixed reactor case which then increases acoustic radiation. In order to verify this hypothesis, analyses were carried out in two steps, as shown in Fig. 4.

Step 1: the same conditions were established for the current, material, and other factors found in actual operation. The magnetic field was then analyzed, and the electromagnetic force was calculated.

Step 2: the electromagnetic force that was calculated based on the magnetic field analysis was mapped for the cross section of each gap. The vibration was then analyzed to calculate the vibration levels.

Appropriate models were created for each analysis, and the electromagnetic force that was calculated in the magnetic field analysis was carried over to the vibration analysis using a software that was specially developed for the purpose.

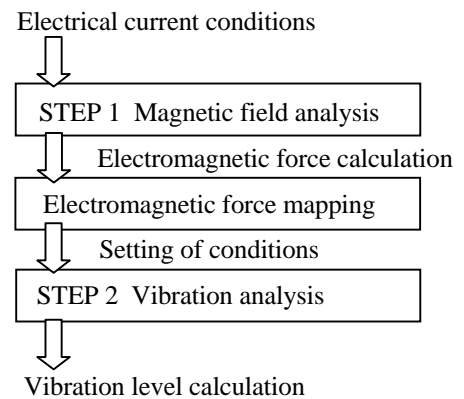


Fig.4 Analysis Procedure

### A. Magnetic Field Analysis

In light of the symmetrical nature of the reactor's shape, only one-eighth of it was modeled in three dimensions, as shown in Fig. 5. The electromagnetic force in the gap was calculated by applying the current conditions shown in Fig. 6.

The actual iron core of the reactor is a layered core made of thin, stacked steel sheets, with adhesive inserted into the gaps to secure the gap material. The four types of magnetic field analysis models shown below were created to ascertain the necessity of modeling these elements. TABLE II summarizes the models, Fig.7 shows schematic drawings of the models, and TABLE III describes the analytical conditions for each model.

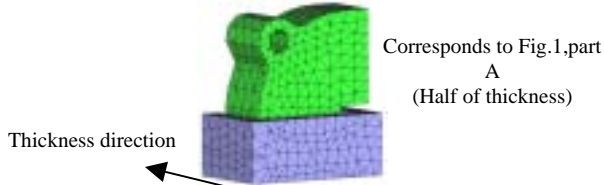


Fig.5 Reactor Analysis Model(1/8area)

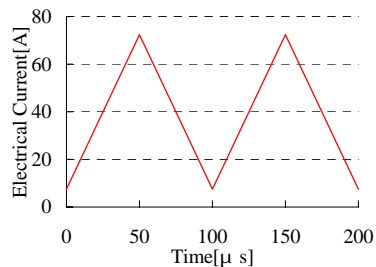


Fig.6 Electrical Current Conditions

TABLE II. MODEL OUTLINE

	imitated lamination	Stacking ratio	Adhesives
<b>Model A</b>			-
<b>Model B</b>	-	-	-
<b>Model C</b>	-		-
<b>Model D</b>	-		

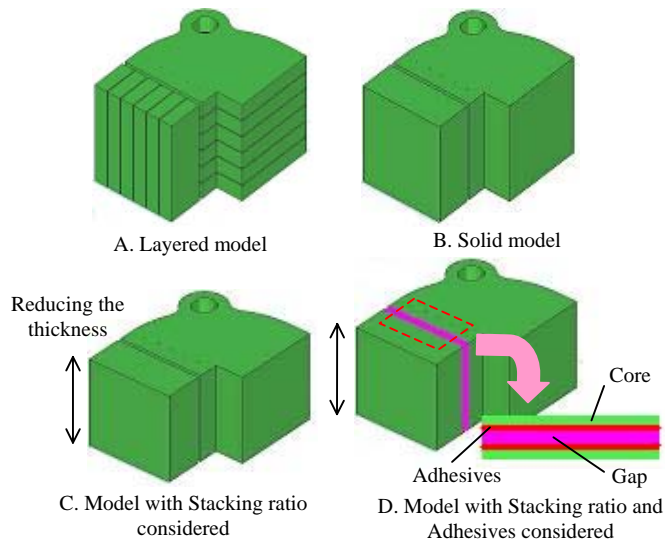


Fig.7 Schematic drawings of the Model

TABLE III. ANALYSIS CONDITIONS

part	Relative magnetic permeability	Material property	B-H characteristic	Remarks
<b>Core</b>		Magnetic substance	Non-linear	
<b>Gap material</b>	1	Non-magnetic substance	Linear	
<b>Adhesives</b>	1	Non-magnetic substance	Linear	Thickness: 0.1mm
<b>Coil</b>	1	Non-magnetic substance	Linear	
<b>Air</b>	1	Non-magnetic substance	Linear	
<b>Lamination</b>	1	Non-magnetic substance	Linear	

### B. Vibration Analysis

Based on the results of the electromagnetic force analysis described above, an exciting force was applied to the reactor gap and the vibration level was measured. The core was modeled as a solid element, and the bracket and band were modeled as shell elements.

Because the rigidity of the coil is one-tenth or less of that of the other parts, its effect on the high-frequency vibration analysis is small. Thus it was not modeled.

The Vibration analysis model is shown in Fig. 8, and the analysis conditions are shown in TABLE IV.

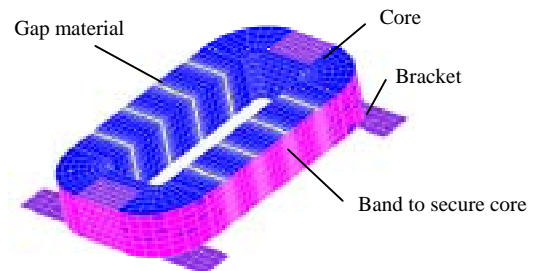


Fig.8 Vibration Analysis model

TABLE IV. VIBRATION ANALYSIS CONDITIONS

Part	Material	Young's modulus [GPa]	Poisson's ratio	Density [kg/m <sup>3</sup> ]
<b>Core</b>	Ferrosilicon sheet	210	0.3	7850
<b>Bracket</b>	Aluminum	71	0.33	2760
<b>Band</b>	Stainless steel	210	0.3	7850
<b>Gap material</b>	Glass epoxy resin	20	0.3	1850

#### IV. VERIFICATION OF ANALYSIS RESULTS

##### A. Results of Magnetic Flux Density and Electromagnetic Force Comparisons

The calculated amplitude of the electromagnetic force for each location in the gap was compared to actual measurements. (See Fig. 9 for the measured locations.) The magnetic flux density is the mean value for the entire cross section, while the electromagnetic force is the total for the cross section.

The magnetic flux density was measured by means of a search coil, while a piezoelectric load cell was used to measure the electromagnetic force. Fig. 10 compares actual measurements of the distribution of magnetic flux density in the gap with the results of the analysis. Figs. 11 and 12 show the mean magnetic flux density and electromagnetic force in the gap when the converter is in operation. TABLE V summarizes the results of magnetic field analysis for each model, together with actual measurements.

The measurements of the magnetic flux density distribution in the gap show a deviation from the mean value that is within three percent, so the distribution is nearly uniform. It was also noted that for the calculation of the magnetic flux density and electromagnetic force when the converter is in operation, the most accurate model, with an accuracy of 97%, was model D, which takes the adhesive and the stacking ratio of the electromagnetic steel sheets into consideration. It can therefore be said that an analytical method that uses a model that takes the adhesive and the stacking ratio into consideration is appropriate.

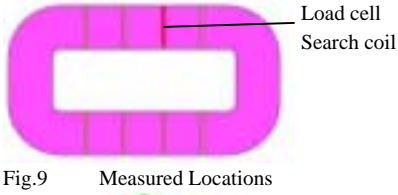


Fig.9 Measured Locations

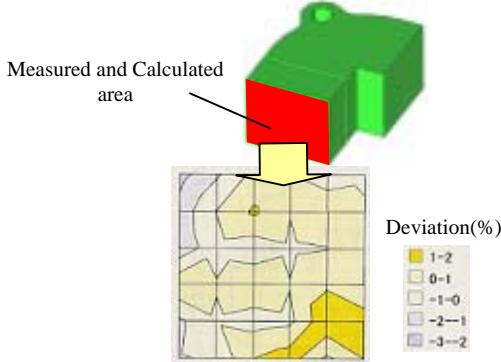


Fig.10a Magnetic flux density distribution (at 70A, Measured result)

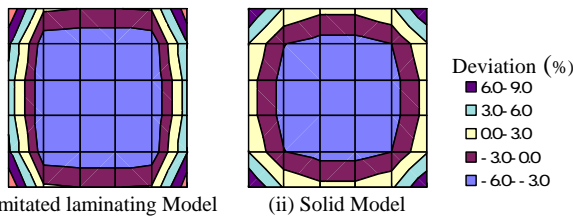


Fig.10b Magnetic flux density distribution (at 70A, Analysis result)

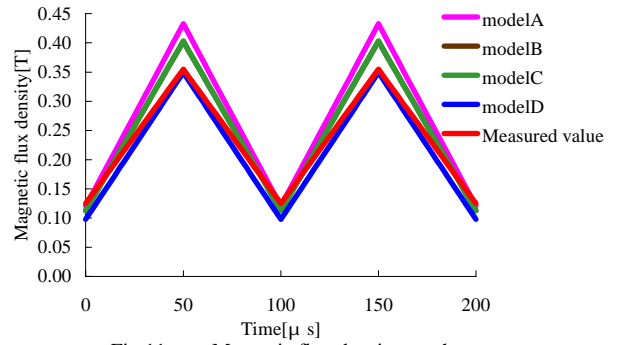


Fig.11 Magnetic flux density graph

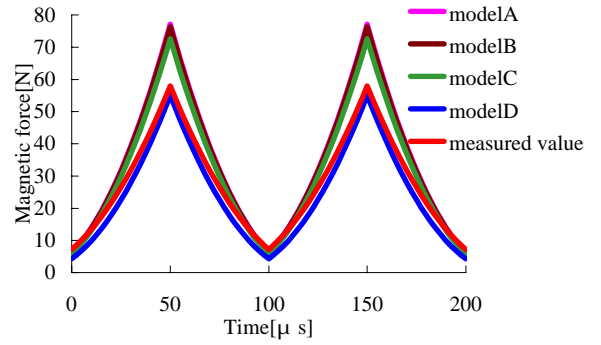


Fig.12 Magnetic force graph

TABLE V. ELECTROMAGNETIC FORCE COMPARISON

(Current Frequency : 10kHz)

Model shape		Model A	Model B	Model C	Model D	Measured value
Magnetic flux density [T]	Maxi mum	0.43	0.40	0.40	0.35	0.36
	Mini mum	0.12	0.11	0.11	0.10	0.13
	Diffe rence	0.31 (135%)*	0.29 (126%)*	0.29 (126%)*	0.25 (109%)*	0.23
Electro magnetic force [N]	Maxi mum	77.2	76.3	72.6	55.1	58.0
	Mini mum	6.1	6.0	5.7	5.8	7.2
	Diffe rence	71.1 (140%)*	70.3 (138%)*	66.9 (131%)*	49.31 (97%)*	50.8

Accuracy : Analysis result / Measured result

##### B. Results of Vibration Mode and Level Comparisons

The analysis results for the vibration mode and vibration level of the reactor were compared to the actual measurements. The measurements were taken with the converter actually operating at the current shown in Fig. 6. Figs. 13 shows a comparison of the analysis results with the measurements. It can be seen that the analysis results for the amounts of displacement in each location and the vibration mode match the measurements almost perfectly. With respect to the vibration mode, as shown in Fig. 13, both the analysis and the measurements indicate that deformation is mainly in the X-axis direction. It was also confirmed that the reactor as a whole is slightly deformed by the force of electromagnetic attraction in the gaps, and that as the force of electromagnetic attraction diminishes when the converter is switched off, the entire reactor is significantly deformed by spring force in the X-axis direction. The results for vibration level, shown in Fig. 14,

indicate that at a frequency of 10 kHz, the level can be analyzed with an error of only about 2 dB.

Note that the measurement points are circled in red in Fig. 13a.

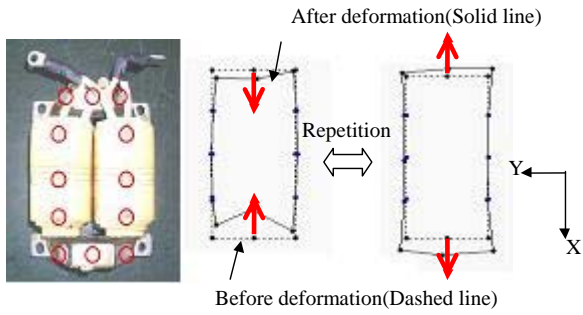


Fig.13a Vibration Mode Measurement Results

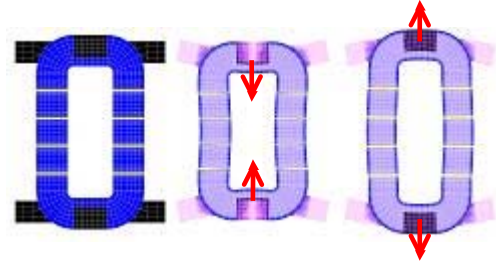


Fig.13 b Vibration Mode Measurement Results

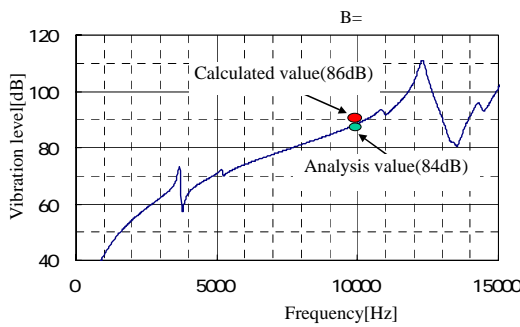


Fig.14 Comparison of Vibration Levels

### C. Summary of Coupled Analysis Results

The results of a coupled analysis between magnetic field and vibration match the measured results well for both electromagnetic force and vibration behavior. Thus, the technique is applicable.

The fact that the calculated vibration behavior matches the measurements also indicates that the initial hypothesis is correct: Vibration is in fact generated when the fluctuation in electromagnetic force across the gaps acts as an excitatory force to propagate vibration in the fixed reactor case, giving rise to acoustic radiation. Also, as shown in Fig. 13, it has been made clear that the direction in which the electromagnetic force acts matches the distinctive vibration mode of the reactor and magnifies the amplitude of the vibration.

## V. STUDY OF IMPROVEMENTS

### A. Cause of Noise and Countermeasures

The analytical technique described here was used to study improvements of the reactor shape. In light of the results above, guidelines were adopted to design a shape that facilitates the following countermeasures:

- (1) The direction in which the electromagnetic force acts shall be diverted.
- (2) There shall be no specific direction with specific vibration characteristics.

In addition, a triangular core like that shown in Fig. 15 was devised taking feasibility considerations (the winding direction of the coil) into account. With this shape, there is no specific direction with specific vibration characteristics, and the direction of the electromagnetic force is diverted by 120 degrees, so a lower noise level can be expected.

Fig. 16 shows the results of an analysis of this shape that was carried out using the analytical technique described above. It is predicted that at a carrier frequency of 10 kHz, the vibration level can be reduced by approximately 22 dB from that of the conventional shape.



Fig.15 Triangular Reactor

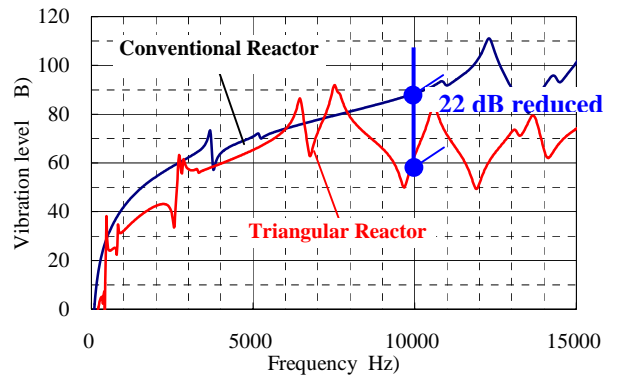


Fig.16 Prediction calculation of an Vibration level

### B. Results of Countermeasures

Based on the approach described in the preceding section, a prototype reactor was experimented and evaluated (Fig. 17). When the vibration amplitude level was measured and compared to the level for the conventional shape, it was seen to have declined by approximately 22 dB.



Fig.17 experimented and evaluated device

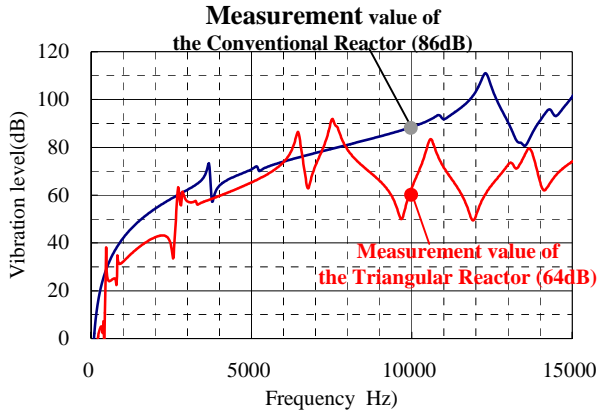


Fig.18 Comparison of an Vibration experiment

## VI. CONCLUSION

A coupled analysis of the magnetic field and vibration behavior in a hybrid vehicle reactor has made it possible to analyze vibration levels in the high-frequency range (5 to 10 kHz), which has not been done before.

In addition, the analytical technique was used to establish that the cause of noise is the fluctuation in electromagnetic force in the reactor gaps, and to develop a new reactor shape that reduces noise. A noise reduction of 12 decibels was achieved.

Additional studies are planned for the near future on the following points:

- Analyzing loss

## ACKNOWLEDGEMENT

We would like to acknowledge the Hiroshi Yoshimoto of TOYOTA TECHNO SERVICE Co, Ltd. For his guidance and support in the course of this research.

## REFERENCES

- [1] Syuya Hagiwara, "VIBRATION ANALYSIS OF A LARGE CAPACITY SHUNT REACTOR", IEEE PAS, Vol101, No3, pp.737-735, 1982
- [2] Yasuro Hori, "Recent Vibration and Noise Reduction Technologies of Substation Equipments", IEEJ-B, Vol 115, No2, pp 101-104, 1995
- [3] Toshiyuki Yanari, "The Present Condition and the Trend of Noise Control Technology of a Stillness Machine", Stillness Machine Noise Control Technical Investigation Special Committee, pp13-44, 48-53, 1996
- [4] Hideo Yamashita, "Acoustic Noise and Loss Reduction of Shunt Reactors", IEEJ-B, Vol104, No12, pp849-856, 1984